



## Molecular Crystals and Liquid Crystals Science and Technology. Section A. Molecular Crystals and Liquid Crystals

Publication details, including instructions for authors and  
subscription information:

<http://www.tandfonline.com/loi/gmcl19>

### Characterization of Organic Epitaxial Films by Atomic Force Microscopy

Hirokazu Tada<sup>a</sup> & Shinro Mashiko<sup>a</sup>

<sup>a</sup> Kansai Advanced Research Center, Communications Research  
Laboratory, 588-2 Iwaoka, Nishi-ku, Kobe, 651-24, Japan

Version of record first published: 24 Sep 2006.

To cite this article: Hirokazu Tada & Shinro Mashiko (1995): Characterization of Organic Epitaxial  
Films by Atomic Force Microscopy, Molecular Crystals and Liquid Crystals Science and Technology.  
Section A. Molecular Crystals and Liquid Crystals, 267:1, 145-150

To link to this article: <http://dx.doi.org/10.1080/10587259508033986>

PLEASE SCROLL DOWN FOR ARTICLE

Full terms and conditions of use: <http://www.tandfonline.com/page/terms-and-conditions>

This article may be used for research, teaching, and private study purposes. Any  
substantial or systematic reproduction, redistribution, reselling, loan, sub-licensing,  
systematic supply, or distribution in any form to anyone is expressly forbidden.

The publisher does not give any warranty express or implied or make any representation  
that the contents will be complete or accurate or up to date. The accuracy of any  
instructions, formulae, and drug doses should be independently verified with primary  
sources. The publisher shall not be liable for any loss, actions, claims, proceedings,  
demand, or costs or damages whatsoever or howsoever caused arising directly or  
indirectly in connection with or arising out of the use of this material.

## CHARACTERIZATION OF ORGANIC EPITAXIAL FILMS BY ATOMIC FORCE MICROSCOPY

HIROKAZU TADA and SHINRO MASHIKO

Kansai Advanced Research Center, Communications Research Laboratory,  
588-2 Iwaoka, Nishi-ku, Kobe 651-24, Japan

**Abstract** The initial stage of the epitaxial growth of vanadyl-phthalocyanine (VOPc) films on alkali halides (AH) and  $\text{MoS}_2$  was studied by atomic force microscopy. Each grain grew epitaxially on the surface with its crystal axis parallel to that expected from the molecular arrangements determined by reflection high energy electron diffraction. The growth mode of the VOPc films on AH was the Volmer-Weber type. Although the height of the grains increased with the deposition time, the grains hardly enlarged in the lateral direction. The shape of grains was affected even by steps with atomic height on AH. On the other hand, the nuclei grew rapidly in the lateral direction on  $\text{MoS}_2$ . The diffusion length of VOPc on  $\text{MoS}_2$  was estimated to be six times as long as that on KBr at room temperature. Large domains with flat surfaces were observed on a  $\text{MoS}_2$  surface when the substrate temperature was kept at 100 °C during film growth.

### INTRODUCTION

Epitaxial films of organic materials grown on inorganic substrates have the potential to be used to build future opto-electronic devices. Among the various organic compounds, metal-phthalocyanine (MPc) is one of the most promising materials for such devices. Molecular arrangements in epitaxial MPc films on various substrates have long been investigated by transmission electron diffraction (TED)<sup>1-6</sup> and reflection high energy electron diffraction (RHEED).<sup>7-10</sup> In addition to the structural information, a systematic investigation of surface morphology and nucleation mechanisms under various growth conditions is essential for the application of organic films. Atomic force microscopy (AFM) is one of the most useful ways to investigate the initial stage of the epitaxial growth of organic materials. In the present article, we will show AFM images of epitaxial films of vanadyl-phthalocyanine (VOPc) grown on KBr, KCl and  $\text{MoS}_2$  under various growth conditions.

Figures 1(a), (b) and (c) show the possible molecular arrangements of VOPc on KBr, KCl and  $\text{MoS}_2$ , respectively.<sup>8,9</sup> The dashed lines in each figure show the surface unit meshes determined by RHEED. VOPc molecules were found to form square lattices on these substrates with intermolecular distances of about 1.4 nm. Although these molecular arrangements were not affected by the growth conditions in the present study, the morphology of the films was strongly affected as will be shown in the following sections.

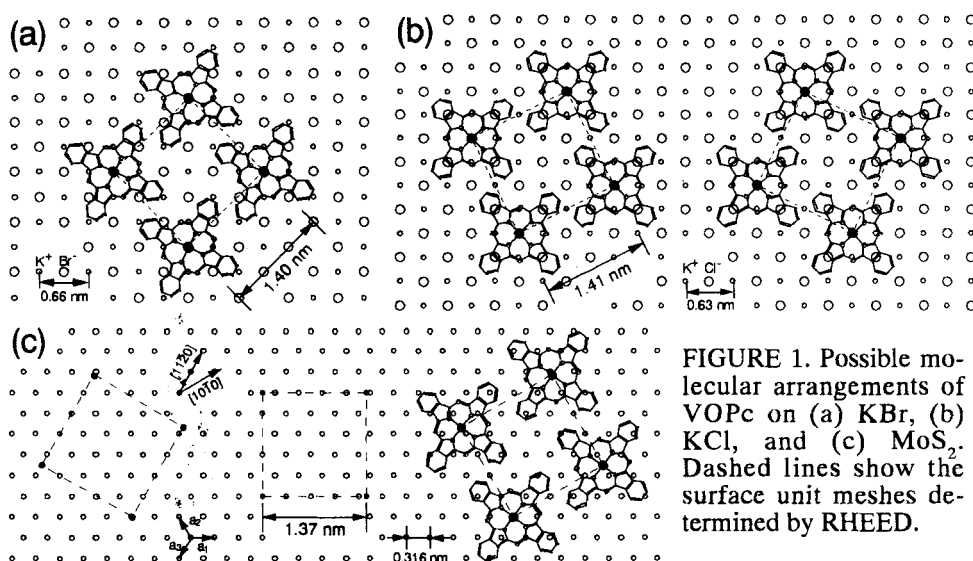


FIGURE 1. Possible molecular arrangements of VOPc on (a) KBr, (b) KCl, and (c) MoS<sub>2</sub>. Dashed lines show the surface unit meshes determined by RHEED.

## EXPERIMENTAL

Film growth was carried out in an ultrahigh vacuum chamber with a base pressure of  $2 \times 10^{-7}$  Pa. The (001) faces of KBr and KCl and the (0001) face of MoS<sub>2</sub> were obtained by air cleaving of the single crystals and natural molybdenite. The substrates were then immediately put into the vacuum chamber. Commercial VOPc powder (Kanto Chemical) was purified by vacuum sublimation. The purified specimen was charged into a Knudsen cell. The film growth rate was monitored with a quartz oscillator located near the specimen holder. The growth rate was controlled to be about 0.3 MLE/min for KBr substrates at room temperature. Here, MLE stands for the number of molecules necessary to cover a KBr surface with the molecular arrangement shown in Fig. 1(a). The molecular flux to attain this growth rate was used as the standard value in the present experiments, and it was 0.3 MLE(KBr)/min. The molecular arrangements were checked to be the same as those shown in Figs. 1 by RHEED with a 20 keV incident electron beam.

The surface structures of the substrates and the grown films were investigated in air by tapping-mode AFM (Digital Instruments Nanoscope III) just after taking them out of the vacuum chamber.

## RESULTS AND DISCUSSION

### AFM images of the substrate surfaces

Figure 2 shows AFM images ( $5 \times 5 \mu\text{m}^2$ ) of as-cleaved KBr(001) faces. Figure 2(a) clearly shows that there are many atomic steps along the  $\langle 100 \rangle$  axes. However steps like

those in Fig. 2(b) were often observed in the images. This is probably due to the deliquescence of KBr. The height of the steps is approximately equal to the value of the lattice constant of

KBr (0.66 nm) or the half of that value in most cases. Similar images were observed for the KCl substrates. On the other hand, most of the images of as-cleaved  $\text{MoS}_2$  showed no steps in the a  $10 \times 10 \mu\text{m}^2$  area.

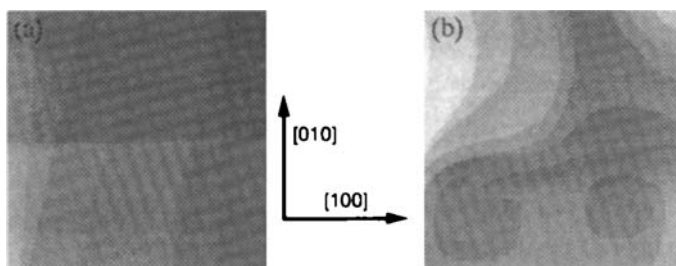


FIGURE 2. AFM images ( $2 \times 2 \mu\text{m}^2$ ) of an as-cleaved KBr(001) surface.

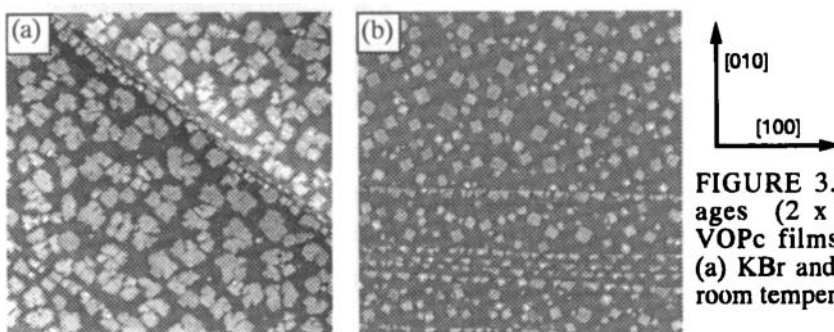


FIGURE 3. AFM images ( $2 \times 2 \mu\text{m}^2$ ) of VOPc films grown on (a) KBr and (b) KCl at room temperature.

#### VOPc films on alkali halides

Figures 3(a) and (b) show AFM images ( $2 \times 2 \mu\text{m}^2$ ) of VOPc grains grown on KBr and KCl, respectively. The substrates were kept at room temperature during film growth. The molecular flux was 0.3 MLE(KBr)/min and the deposition time was 20 min. The shape of the grains is almost a rectangular parallelepiped. The side faces of the grains on KBr are parallel to the  $\langle 110 \rangle$  axes and those on KCl are parallel to the  $\langle 210 \rangle$  axes of the substrates. This means that the grains grow from the nuclei having the lattices shown in Figs. 1(a) and (b).

Figure 4 shows an AFM image ( $5 \times 5 \mu\text{m}^2$ ) of a VOPc film grown on KBr at room temperature at a rather slow growth rate. The molecular flux was 0.03 MLE(KBr)/min and the deposition time was 200 min. Most grains are located at the step edges with few grains on the terrace. This indicates that the stable nucleus is generated not by physisorption of one molecule on the surface but by cluster forma-

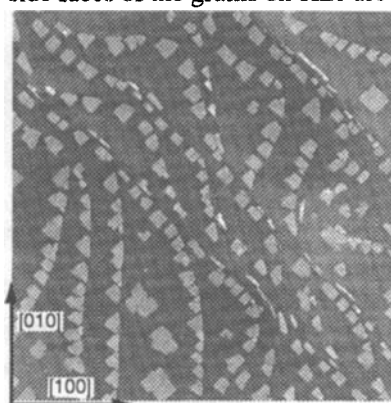


FIGURE 4. AFM image ( $5 \times 5 \mu\text{m}^2$ ) of a VOPc film grown on KBr with a slow growth rate.

tion via collision between molecules during surface migration.

The grain density decreased and each grain enlarged with increasing substrate temperature as was expected. Figure 5 shows an AFM image ( $5 \times 5 \mu\text{m}^2$ ) of a VOPc film grown on KBr that was kept at  $100^\circ\text{C}$  during film growth. The height of the grains ranges from 25 to 40 nm. The surface of the topmost layers is rather flat. The side faces are perpendicular to the substrate surface and most of them are parallel to the  $\langle 110 \rangle$  axes. Some are parallel to steps whose height is at most 0.6 nm. It is interesting that the grain shape is affected by steps even of atomic height.

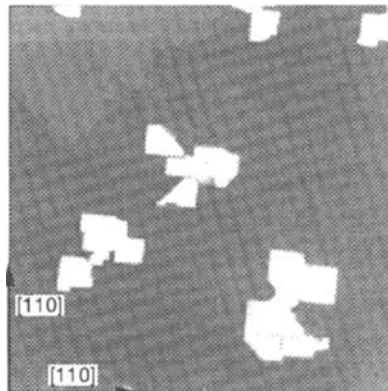


FIGURE 5. AFM image of a VOPc film on KBr at  $100^\circ\text{C}$  ( $5 \times 5 \mu\text{m}^2$ ).

#### VOPc films on $\text{MoS}_2$

Figure 6(a) shows an AFM image ( $5 \times 5 \mu\text{m}^2$ ) of the very initial stage of VOPc film growth on  $\text{MoS}_2$  at room temperature. The molecular flux was 0.3 MLE(KBr)/min and the deposition time was 3 min. The grains are almost rectangular. The crystal axis of grains rotates approximately every  $60^\circ$ , which indicates the grains grow from the nuclei shown in Fig. 1(c). The height of each domain is about 0.5 nm.

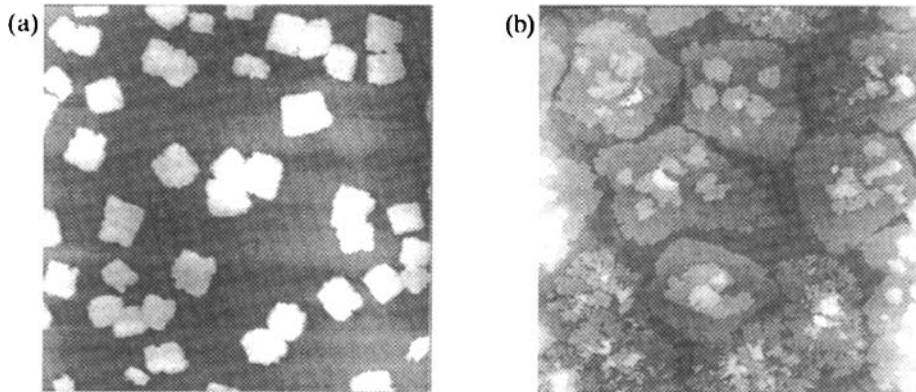


FIGURE 6. AFM images ( $5 \times 5 \mu\text{m}^2$ ) of VOPc films on  $\text{MoS}_2$  at room temperature with the deposition time of (a) 3 min and (b) 20 min.

The grains enlarged in the lateral direction with a subsequent 20-min deposition and fused together as shown in Fig. 6(b). The grains consist of two layers with islands on the topmost layer. These islands will fuse together with increasing deposition time in a manner similar to the formation of the underlying layers. The height difference between each layer is about 0.8 nm, which is larger than the height of a molecule with parallel molecular orientation. Since the molecules were found to form square lattices till the film thickness

reaches 10 MLE from the RHEED analysis (Fig. 1(c)), it is difficult to imagine that the molecular planes are inclined. Each layer may consist of two molecular layers in which the molecules form body-centered or face-centered tetragonal lattices.

Figure 7 shows an AFM image ( $10 \times 10 \mu\text{m}^2$ ) of a VOPc film on  $\text{MoS}_2$  that was kept at  $100^\circ\text{C}$  during growth. The grains are large and have flat surfaces. The area labeled A is the uncovered surface of  $\text{MoS}_2$ . The first VOPc layer covered the large area marked B. Areas C and D denote grains consisting of two and three layers, respectively. The VOPc film is thought to grow in a layer-by-layer fashion on  $\text{MoS}_2$ .

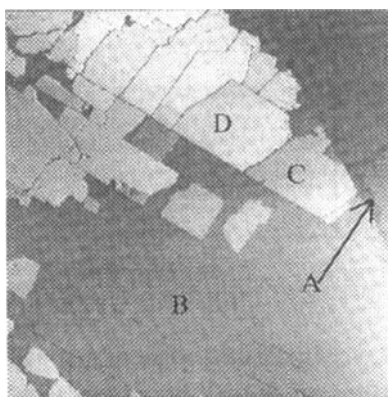


FIGURE 7. AFM image ( $10 \times 10 \mu\text{m}^2$ ) of a VOPc film grown on  $\text{MoS}_2$  at  $100^\circ\text{C}$ .

#### Estimation of the diffusion length and the saturation density of grains

In the case of the VOPc film growth on AH, the grain density and the total area covered with grains reached a saturation point, although the height of the grains increased with the deposition time. This is a typical model of Valmer-Weber type film growth. On the other hand, the nuclei grew rapidly in the lateral direction on  $\text{MoS}_2$ . The molecules migrate on the surface sufficiently to merge with the grains since they are held on the surface via weak van der Waals interaction and there are few steps on  $\text{MoS}_2$ . Almost the layer-by-layer growth (Frank-van der Merwe type film growth) can be almost perfectly achieved under appropriate growth conditions. This difference in the growth mode comes from the difference in the diffusion length of VOPc on surfaces. The diffusion length is estimated quantitatively according to the model introduced by Lewis and Campbell.<sup>11</sup>

Taking into account the desorption of the molecules during migration, the density of grains,  $n_s$ , is given as the function of the deposition time,  $t$ :

$$n_s = N_s \left\{ 1 - \exp\left(-\frac{I}{N_s}t\right) \right\} \quad \text{or} \quad \log(N_s - n_s) = -\frac{I}{N_s}t.$$

Here,  $N_s$  is the saturation nucleus density and  $I$  is the nucleation rate. The diffusion length,  $d$ , can be estimated by using  $N_s$ :

$$d = \frac{1}{\sqrt{N_s}}.$$

Figure 8(a) plots of the number of grains per  $1 \mu\text{m}^2$  ( $n_s$ ) on KBr versus the deposition time ( $t$ ). The molecular flux was  $0.3 \text{ MLE(KBr)/min}$  and the substrate was kept at room temperature. It is possible to evaluate both  $N_s$  and  $I$  from the intercept and slope of the straight line fitted to the plot of  $\log(N_s - n_s)$  versus  $t$  as shown in Fig. 8(b). The values of  $N_s$ ,  $I$  and  $d$  were  $74 \mu\text{m}^{-2}$ ,  $1.2 \mu\text{m}^{-2}\text{s}^{-1}$  and  $0.12 \mu\text{m}$ , respectively.

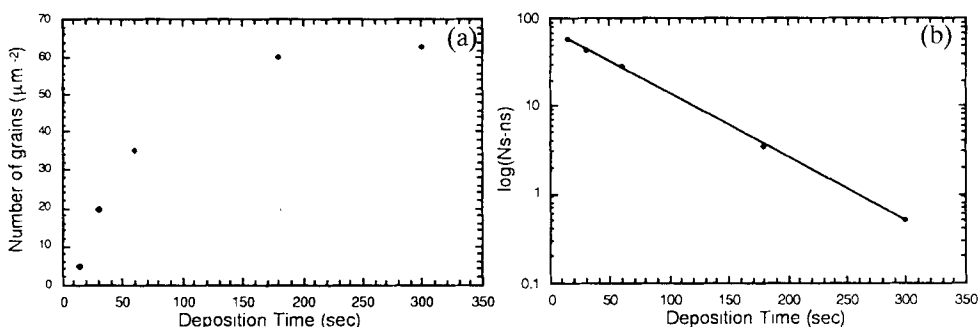


FIGURE 8. Plot of (a)  $n_s$  versus  $t$  and (b)  $\log(N_s - n_s)$  versus  $t$ .

In the case of the film growth on  $\text{MoS}_2$ , it is difficult to measure the grain density, since the grains fuse together with the deposition time. From the highest grain density of  $1.8 \mu\text{m}^{-2}$  at the very initial stage, the diffusion length was estimated to be  $0.75 \mu\text{m}$  for VOPc molecules on  $\text{MoS}_2$  at room temperature. This value is six times as large as that on a KBr substrate.

## CONCLUSION

An AFM study of epitaxial film growth of VOPc on AH and  $\text{MoS}_2$  has revealed: (1) multiple nuclei formation in each case; (2) the crystal axis of each grain is parallel to that expected from the molecular arrangements determined by RHEED; (3) the growth mode of VOPc films on AH is the Volmer-Weber type; (4) the shape of grains is affected by atomic steps on AH; (5) cluster formation from collisions between molecules during migration is essential to nucleation; (6) the nuclei grow rapidly in the lateral direction on  $\text{MoS}_2$ ; (7) large domains with flat surfaces can be obtained on  $\text{MoS}_2$  at  $100^\circ\text{C}$ ; and (8) the diffusion length of VOPc on  $\text{MoS}_2$  is about six times as long as that on KBr at room temperature.

## REFERENCES

1. E. Suito, N. Uyeda, and M. Ashida, *Nature*, **194**, 273 (1962).
2. M. Ashida, *Bull. Chem. Soc. Jpn.*, **39**, 2625 (1966).
3. H. Saijo, T. Kobayashi, and N. Uyeda, *J. Cryst. Growth*, **40**, 118 (1977).
4. H. Yanagi, T. Kouzeki, and M. Ashida, *J. Appl. Phys.*, **73**, 3812 (1993).
5. A. J. Dann, H. Hoshi, and Y. Maruyama, *J. Appl. Phys.*, **67**, 1371 (1990).
6. H. Hoshi and Y. Maruyama, *J. Appl. Phys.*, **69**, 3046 (1991).
7. M. Hara, H. Sasabe, A. Yamada, and A. F. Garito, *Jpn. J. Appl. Phys.*, **28**, L306 (1989).
8. H. Tada, K. Saiki, and A. Koma, *Jpn. J. Appl. Phys.*, **30**, L306 (1991).
9. H. Tada, T. Kawaguchi, and A. Koma, *Appl. Phys. Lett.*, **61**, 2021 (1992).
10. G. E. Collins, K. W. Nebesny, C. D. England, L. -K. Chan, P. A. Lee, B. A. Parkinson, and N. R. Armstrong, *J. Vac. Sci. Tech. A*, **10**, 2902 (1992).
11. B. Lewis and D. S. Campbell, *J. Vac. Sci. Tech.*, **4**, 209 (1967).